Bioorganic & Medicinal Chemistry 17 (2009) 74–84

Contents lists available at ScienceDirect

Bioorganic & Medicinal Chemistry

journal homepage: www.elsevier.com/locate/bmc

Discovery of novel analgesic and anti-inflammatory 3-arylamine-imidazo[1,2-*a*]pyridine symbiotic prototypes

Renata B. Lacerda [a,b], Cleverton K. F. de Lima [a,c], Leandro L. da Silva [a,c], Nelilma C. Romeiro [a], Ana Luisa P. Miranda [a,c], Eliezer J. Barreiro [a,b,c], Carlos A. M. Fraga [a,b,c,*]

[a] *Laboratório de Avaliação e Síntese de Substâncias Bioativas (LASSBio), Faculty of Pharmacy, Federal University of Rio de Janeiro, PO Box 68023, 21941-902, Rio de Janeiro, RJ, Brazil*
[b] *Programa de Pós-Graduação em Química, Chemistry Institute, Federal University of Rio de Janeiro, Rio de Janeiro, RJ, Brazil*
[c] *Programa de Pós-Graduação em Farmacologia e Química Medicinal, Institute of Biomedical Sciences, Federal University of Rio de Janeiro, Rio de Janeiro, RJ, Brazil*

ARTICLE INFO

Article history:
Received 13 September 2008
Revised 7 November 2008
Accepted 8 November 2008
Available online 17 November 2008

Keywords:
3-Arylamine-imidazo[1,2-*a*]pyridines
p38 MAPK
Analgesic
Anti-inflammatory
Symbiotic drugs

ABSTRACT

We describe herein the design, synthesis and pharmacological evaluation of novel 3-arylamine-imidazo[1,2-*a*]pyridine derivatives structurally designed as novel symbiotic prototypes presenting analgesic and anti-inflammatory properties. The derivatives obtained were submitted to in vivo assays of nociception, hyperalgesia and inflammation, and to in vitro assays of human PGHS-2 inhibition. These assays allowed the identification of compound LASSBio-1135 (**3a**) as an anti-inflammatory and analgesic symbiotic prototype. This compound inhibited moderately the human PGHS-2 enzyme activity (IC_{50} = 18.5 μM) and reverted the capsaicin-induced thermal hyperalgesia (100 μmol/kg, po) similarly to p38 MAPK inhibitor SB-203580 (**2**). Additionally, LASSBio-1135 (**3a**) presented activity similar to celecoxib (**1**) regarding the reduction of the carrageenan-induced rat paw edema (33% of inhibition at 100 μmol/kg, po). We also discovered derivatives LASSBio-1140 (**3c**) and LASSBio-1141 (**3e**) as analgesic and anti-inflammatory prototypes, which were able to attenuate the capsaicin-induced thermal hyperalgesia (100 μmol/kg, po) and reduce the carrageenan-induced paw edema (ED_{50} = 11.5 μmol/kg (3.3 mg/kg) and 14.5 μmol/kg (4.1 mg/kg), respectively), being both more active than celecoxib (**1**), despite the fact that their effects involve a different mechanism of action. Additionally, derivative LASSBio-1145 (**3j**) showed remarkable analgesic (ED_{50} = 22.7 μmol/kg (8.9 mg/kg)) and anti-inflammatory (ED_{50} = 8.7 μmol/kg (3.4 mg/kg)) profile in vivo (100 μmol/kg; po), in AcOH-induced abdominal constrictions in mice and carrageenan-induced rat paw edema models, respectively, being a novel orally-active anti-inflammatory drug candidate that acts as a selective PGHS-2 inhibitor (IC_{50} = 2.8 μM).

1. Introduction

Inflammation is a complex defensive process that may vary from a localized to a generalized response characterized by the accumulation of local fluids and leukocytes with the objective of eliminating the noxious stimulus. The inflammatory response occurs in three distinct temporal phases, which seems to be mediated by different physiological and immunological phenomena: the acute phase, characterized by the transient local vasodilatation and the increase of the capillary permeability; a delayed sub-acute phase characterized by the infiltration of leukocytes and other phagocytising cells; and the proliferative chronic phase, in which occurs degeneration of the affected tissue and fibrosis.[1]

The acute inflammation occurs as the initial response to tissue injury, being mediated by the release of autacoids, for example, histamine, serotonin, bradikynin, prostaglandins and leukotrienes, and preceding the development of an immune response. On the other hand, the chronic inflammatory process involves the release of diverse mediators which do not have significant participation in the acute phase, as interleukins, interferon and tumor necrosis factor α (TNF-α, a cytokine that plays a major role in this kind of inflammatory process and whose production is associated with some difficultly treatable diseases, for example, rheumatoid arthritis, Crohn's disease, among others.[2]

Although the efficacy of selective PGHS-2 enzyme inhibitors has been proved, and these drugs together with the classical non-selective NSAIDs constitute the mainstay of symptomatic treatment of many inflammatory disorders and soft-tissue injuries, the results of two major prospective studies—the VIGOR (Vioxx Gastrointestinal Outcomes Research Study) and APPROVe (Adenomatous Polyp Prevention on Vioxx)—demonstrated an increased risk of serious cardiovascular events, including heart attacks and strokes in patients making use of rofecoxib.[3] This profile suggests that the ideal NSAID does not have to be excessively selective for the PGHS-2 enzyme, for example, celecoxib (**1**), and demonstrates the need for

* Corresponding author. Tel.: +55 21 25626503; fax: +55 21 25626644.
E-mail address: cmfraga@pharma.ufrj.br (C.A.M. Fraga).

0968-0896/$ - see front matter © 2008 Elsevier Ltd. All rights reserved.
doi:10.1016/j.bmc.2008.11.018

searching new strategies and new targets for efficient and safe treatment of the chronic inflammatory diseases.[4]

The interest in the MAP kinase pathway as a potential target for the development of novel anti-inflammatory drugs has grown recently. In fact, the identification of p38 MAPK as the target of some pyridinil-imidazole compounds[5] confirmed the role of this intracellular enzyme in the regulation of many physiological and pathological states and reinforced the importance of its modulation in the therapy of some inflammatory diseases. The clinical assays with the selective p38 inhibitors demonstrate the therapeutic benefits of the blockage of this signaling pathway responsible for the regulation of cytokines production, for example, IL-1β and TNF-α.[6] Moreover, the characterization of the pharmacological profile displayed by the selective p38 inhibitor prototype SB203580 (**2**), proved its disease-modifying activity in the adjuvant-induced arthritis model.[6] This set of results strongly suggests that adequate modulation of production of these cytokines can bring significant benefits to the therapy of chronic inflammatory diseases,[6] for example, rheumatoid arthritis, psoriasis, asthma, chronicle obstructive pulmonary disease (COPD) and Crohn's disease, and has supported the potential use of selective p38 inhibitors as monotherapy[7] or in set with other drugs able to act synergistically.

The combination of two or more clinically validated therapeutic targets with mutual participation in specific multifactorial diseases can represent an interesting strategy to increase the available pharmacological space for the discovery of new drugs.[8] Emerging from this new Medicinal Chemistry approach, the concept of symbiotic drugs appears as an interesting therapeutic innovation in the search for more efficient and safe drugs for treating chronic diseases. A design of these symbiotic agents should be made to allow the molecular recognition of two distinct biological targets, involved in the same disease and belonging to different biochemical pathways, in order to promote the treatment and the prevention of the harmful stimulus amplification more efficiently.[9]

In this context, the present work describes the synthesis and the investigation of the analgesic and anti-inflammatory properties of new 3-arylamine-imidazo[1,2-*a*]pyridine derivatives (**3**) designed as symbiotic agent candidates acting as PGHS-2 and p38 MAP kinase inhibitors. The rational approach exploited in the design of compounds belonging to series (**3**) considered the diarylheterocyclic subunit as a common structural feature of selective inhibitors of both targets,[10] for example, celecoxib (**1**) and SB-203580 (**2**), and led us to propose the combination of their corresponding pharmacophoric groups in a common azahomologue structural pattern, by applying the molecular hybridization strategy[11] (Fig. 1).

The imidazo[1,2-*a*]pyridine ring was chosen as the core heterocyclic scaffold of target compounds (**3**), due to its presence in the pyridazinone p38 MAPK inhibitor (**4**)[12] and also because it can be envisioned as a resultant of the fusion of the imidazole and phenyl rings present in SB-203580 (**2**). Additionally, the anti-inflammatory and antinociceptive activity of some *N*-acylhydrazone derivatives belonging to imidazo[1,2-*a*]pyridine class, for example, 4-bromophenyl derivative (**5**) was previously described by our research group,[13] corroborating the importance of this azaheterocyclic ring for the desired bioprofile (Fig. 1).

The functionalized aromatic rings Ar_1 and Ar_2, for example, 4-(methylsulfonyl)phenyl, 2-pyridinyl, 4-pyridinyl and other isosteric subunits, were elected in order to retain, in just one chemical entity, the characteristic pharmacophoric groups of selective p38 MAPK and PGHS-2 inhibitors, aiming to favor their simultaneous blockage (Fig. 1).

2. Results and discussion

2.1. Chemistry

The new functionalized 3-arylamine imidazo[1,2-*a*]pyridine derivatives (**3a–h**) were synthesized by exploring at the key-step, the three component condensation (3CC) of heterocyclic amidines with aldehydes and isocyanides described by Groebke[14] as a variation of the classic multi-component condensations originally developed by Passerini[15] and Ugi.[16] The synthesis of isocyanides (**6a–d**) was performed in two steps, starting with the formylation of the corresponding aromatic amines (**7a–d**) by refluxing with ethyl formate in triethylamine[17] to produce the corresponding formamides (**8a–d**) in 35–95% yield (Scheme 1). The 2-pyridinil-form-

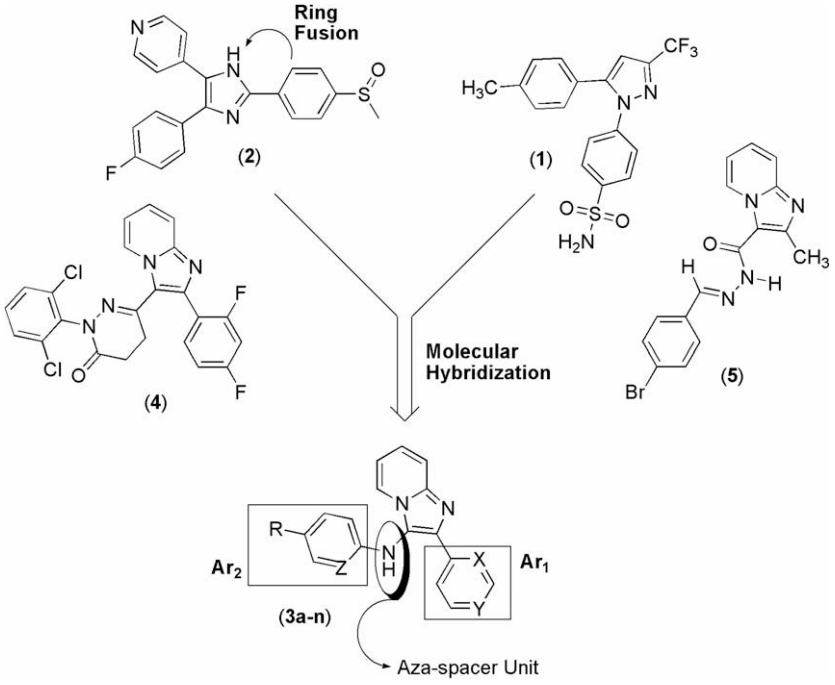

Figure 1. Design concept of new 3-arylamine imidazo[1,2-*a*]pyridine derivatives (**3a**–**n**).

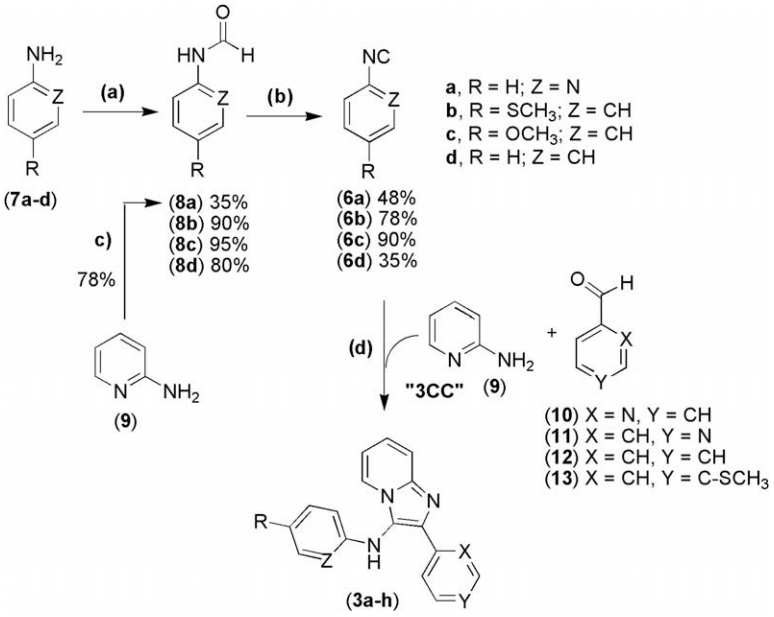

Scheme 1. Reagents and conditions: (a) ethyl formate, Et_3N, reflux, 20–96 h; (b) $POCl_3$, CH_2Cl_2, Et_3N, 0 °C, 2 h; (c) i—HCO_2H, Ac_2O, 50–60 °C, 2 h, ii—2-aminopyridine, ethyl ether, rt, 48 h; (d) AcOH, MeOH, rt, 24 h (see Table 1).

amide derivative (**8a**) obtained in only 35% yield after 96 h could alternatively be prepared in 78% yield through the formylation of 2-aminopyridine (**9**) with the more reactive mixed formylacetyl anhydride generated in situ[18] (Scheme 1).

Afterward, the desired isocyanides (**6a–d**) were obtained in yields varying from 40% to 90%, exploiting the dehydration of corresponding formamides (**8a–d**) by treatment with $POCl_3$ in triethylamine (Scheme 1).[16,17]

The target derivatives 3-arylamine-imidazo[1,2-*a*]pyridine (**3**) were obtained in moderate yields, by applying the multi-component condensation of isocyanides (**6a–d**) with the appropriate aromatic aldehydes (**10–13**) and 2-aminopyridine (**9**) in methanol, under acidic conditions (Scheme 1 and Table 1).[14] Contrary to our expectations, the 3-arylamino imidazo[1,2-*a*]pyridine derivatives presenting 4-pyridinyl ring, that is (**3c**) and (**3d**), were not formed when three-component condensation was performed exploiting 4-pyridinylcarboxaldehyde (**11**) as the electrophilic species. The side-products from these reactions were identified as the corresponding 4-pyridinyl imines (**14**) and (**15**), respectively (Fig. 2), which are probable resulted from condensation of the heteroaromatic aldehyde with the aniline formed due to partial hydrolysis of isocyanides (**6b**) and (**6d**) during the long reaction

Table 1
Yields and physical properties of the 3-arylamino imidazo[1,2-*a*]pyridine derivatives (**3**)

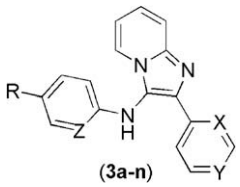

Compound	Ar_1		Ar_2		Molecular formula[a]	M_W	Yield (%)
	X	Y	R	Z			
3a	N	CH	H	CH	$C_{18}H_{14}N_4$	286.33	40
3b	N	CH	SCH_3	CH	$C_{19}H_{16}N_4S$	332.42	40
3c	CH	N	H	CH	$C_{18}H_{14}N_4$	286.33	0 (50)[c]
3d	CH	N	SCH_3	CH	$C_{19}H_{16}N_4S$	332.42	0 (60)[b]
3e	CH	CH	H	CH	$C_{19}H_{15}N_3$	285.34	25
3f	CH	C-SCH_3	H	CH	$C_{20}H_{17}N_3S$	331.43	50
3g	CH	C-SCH_3	OCH_3	CH	$C_{21}H_{19}N_3OS$	361.46	70
3h	CH	C-SCH_3	H	N	$C_{19}H_{16}N_4S$	332.42	50
3i	CH	C-SO_2CH_3	H	CH	$C_{20}H_{17}N_3O_2S$	363.43	60[c]
3j	CH	C-SO_2CH_3	OCH_3	CH	$C_{21}H_{19}N_3O_3S$	393.46	60[c]
3l	CH	C-SO_2CH_3	H	N	$C_{19}H_{16}N_4O_2S$	364.42	80[c]
3m	N	CH	SO_2CH_3	CH	$C_{19}H_{16}N_4O_2S$	364.42	60[c]
3n	CH	N	SO_2CH_3	CH	$C_{19}H_{16}N_4O_2S$	364.42	85[c]

[a] The analytical results for C, H, N, S were within ±0.4% of calculated values.
[b] Yields obtained from alternative two step condensation described in Scheme 2.
[c] Obtained by chemoselective oxidation of the corresponding methylsulfide derivatives (**3b**), (**3d**) and (**3f–h**) as described in Scheme 3.

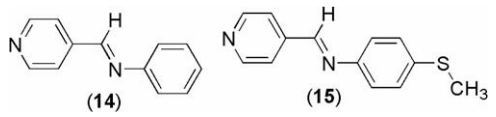

Figure 2. Imine derivatives (**14**) and (**15**) evidenced as the major products obtained from three-component condensation of 4-pyridinylcarboxaldehyde (**11**), 2-aminopyridine (**9**) and phenylisocyanide (**6d**) or 4-methylthiophenylisocyanide (**6b**), respectively.

time of this kinetically unfavorable three-component coupling under acidic conditions.

Given the limitation of classical 3CC methodology to prepare imidazo[1,2-*a*]pyridine derivatives (**3c**) and (**3d**) we decided to apply a two step variation of this reaction, where the imine derivative (**16**) was initially prepared through the condensation of equimolar amounts of 4-pyridinylcarboxaldehyde (**11**) with 2-aminopyridine (**9**) in toluene,[19] followed by the addition of isocyanide derivative (**6b**) or (**6d**) to furnish the desired compounds (**3d**) and (**3c**) in 60% and 50% yield, respectively (Scheme 2 and Table 1).

Finally, the 3-arylamine-imidazo[1,2-*a*]pyridine derivatives (**3b**), (**3d**) and (**3f–h**) with the methylsulfide group attached to Ar_1 or Ar_2 subunits were chemoselectively oxidized to the corresponding sulfones in good yields (60–80%) using Oxone® ($2KHSO_5{\cdot}KHSO_4{\cdot}K_2SO_4$) as the oxidizing agent (Scheme 3 and Table 1).[20]

Although Mandair et al.[21] have reported the possible formation of regioisomers during the construction of functionalized imidazo[1,2-*a*]pyridine ring exploiting the 3CC strategy in a previous work, the regioselective formation of 3-arylamino derivatives was confirmed through 2D-NOESY experiment, which showed the spatial relationship between the hydrogen at the NH group and the hydrogen located at C-5 of the azaheterocyclic ring of derivative (**3b**), impossible to occur in 2-arylamino isomer (Fig. 3).

All new imidazo[1,2-*a*]pyridine derivatives described herein were completely characterized by common spectroscopic methods (see Section 4) and their analytical results for C, H, and N were within ±0.4% of calculated values.

2.2. Analgesic and anti-inflammatory activities

First, we evaluated the in vivo analgesic and anti-inflammatory profile of eight 3-arylamine-imidazo[1,2-*a*]pyridine derivatives (**3a**), (**3c**), (**3e**), (**3i**), (**3j**), (**3l**), (**3m**), (**3n**) elect, presenting pharmacophoric groups for COX-2 and p38 MAPK inhibition, in the acetic acid induced abdominal constrictions[22] in mice and carrageenan-induced rat paw edema (CIRPE),[23] respectively. The new 3-arylamine-imidazo[1,2-*a*]pyridine compounds and celecoxib (**1**), used

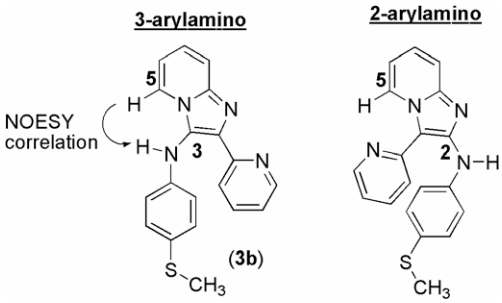

Figure 3. Characterization of 3-arylamino imidazo[1,2-*a*]pyridine regioisomer by NOESY experiment.

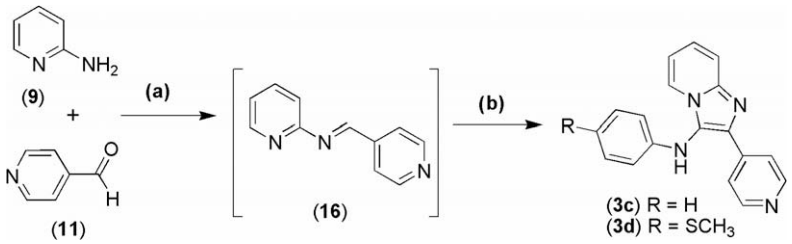

Scheme 2. Reagents and conditions: (a) toluene, 50 °C, 30 min; (b) Ph-NC or 4-H_3CSPh-NC, NH_4Cl, reflux, 30 h (see Table 1).

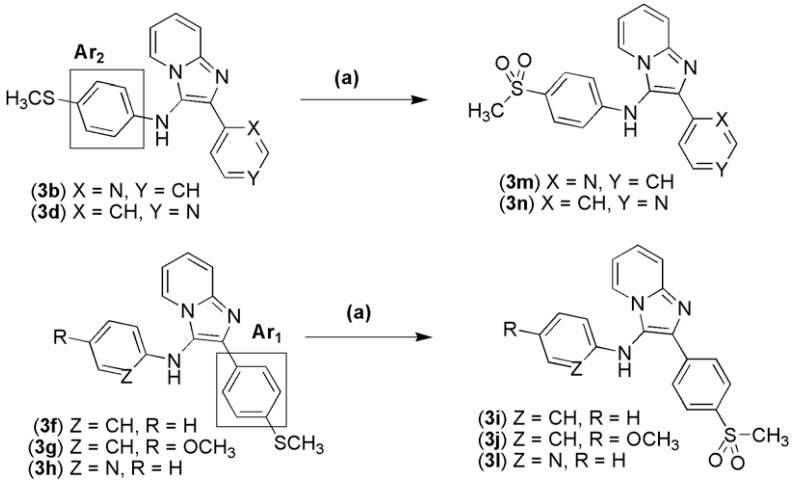

Scheme 3. Reagents and conditions: (a) Oxone®, MeOH, rt, 1 h (see Table 1).

as standard drug, were administered orally at the dose of 100 μmol/kg. The obtained results are disclosed in Tables 2 and 3, respectively.

The analysis of these results led us to conclude that the most active analgesic compound was the arylsulfone derivative (**3j**), which was able to reduce remarkably the AcOH-induced constrictions, presenting 53.0% of inhibition (Table 2). The expressive reduction of the analgesic activity evidenced for Ar_1 aza-substituted analogues (**3m**) and (**3n**), which were both able to reduce the constrictions in ca. 33%, haspointed the pharmacophoric character of the *para*-methoxyphenyl framework for the antinociceptive profile of the imidazo[1,2-*a*]pyridine derivatives of series (**3**). The ED_{50} obtained for compound (**3j**), that is, 22.7 μmol/kg (8.9 mg/kg) (Table 1), showed that, as analgesic agent, it is 10-fold more potent than COX-2 inhibitor celecoxib (**1**).[24]

The anti-inflammatory profile of imidazo[1,2-*a*]pyridine derivatives (**3a**), (**3c**), (**3e**) and (**3i–n**) was then evaluated in the CIRPE test,[23] as described in Table 3.

Compounds (**3i**), (**3a**), (**3c**), (**3e**) and (**3j**) were able to inhibit edema formation significantly and the last three were more active than celecoxib (**1**), the standard anti-inflammatory drug (30% inhibition at 100 μmol/kg). Among the active derivatives, we would like to emphasize (**3e**), which was the most active despite being a non-functionalized derivative, presenting 64% of inhibition of constrictions and an ED_{50} of 14.5 μmol/kg (4.1 mg/kg). On the other hand, the most active analgesic compound (**3j**) presented an ED_{50} of 8.7 μmol/kg (3.4 mg/kg) regarding the anti-inflammatory effect in CIRPE model, proving to be, once again, 10-fold more potent than celecoxib (**1**) (ED_{50} = 87.7 μmol/kg (33.4 mg/kg)).

Considering that the anti-edematogenic profile observed for (**3j**), (**3a**) and (**3e**) could depend at least in part on PGHS inhibition, we decided to perform whole blood in vitro assay[25] to investigate their ability to inhibit isoforms 1 and 2 of the target enzyme. PGHS-1 activity was measured through TXB_2 production in blood samples drawn from donors that had not taken any NSAID for two weeks, while LPS-induced PGHS-2 activity was also determined by TXB_2 plasma levels measured by RIA. None of the tested compounds inhibited the production of TXB_2 derived from PGHS-1 at the concentration of 100 μM, contrary to the behavior observed for celecoxib (**1**), which was able to inhibit it in 53.4% at same molar concentration. The results showed that compounds (**3a**) and (**3j**) were able to inhibit the production of TXB_2 from PGHS-2 with IC_{50} of 18.5 μM and 2.8 μM, respectively (Table 1). On the other hand, compound (**3e**) did not act as PGHS-2 inhibitor, showing that its great anti-inflammatory activity should be dependent on other mechanism of action.

Table 2
Analgesic profile of imidazo[1,2-*a*]pyridine compounds (**3a**), (**3c**), (**3e**) and (**3i–n**) in AcOH-induced abdominal constriction test

Compound	Dose (μmol/kg)	No. of constrictions[a]	Inhibition (%)	ED_{50} (μmol/kg)
Vehicle	—	59.2 ± 1.33	—	—
(**1**) Celecoxib	100	31.9 ± 4.7	46.1*	247.0[c]
(**3a**)	100	61.2 ± 2.9	−3.0 ns[b]	—
(**3c**)	100	51.5 ± 2.3	13.0 ns[b]	—
(**3e**)	100	52.8 ± 2.9	10.8 ns[b]	—
(**3i**)	100	54.8 ± 3.4	7.4 ns[b]	—
(**3j**)	100	27.8 ± 3.7	53.0*	22.7
(**3l**)	100	46.0 ± 1.7	22.2*	—
(**3m**)	100	39.2 ± 3.3	33.7*	—
(**3n**)	100	39.3 ± 3.3	33.6*	—

Compounds were administered orally; $N = 7–10$ animals.
[a] Results expressed in terms of mean ± SEM.
[b] Not statistically significant.
[c] Data obtained from Ref. 24.
* $p < 0.05$ (ANOVA one way followed by Dunnet test).

Table 3
Anti-inflammatory activity of imidazo[1,2-*a*]pyridine derivatives (**3a**), (**3c**), (**3e**) and (**3i–n**) in carrageenan-induced rat paw edema (CIRPE) assay and PGHS-2 inhibitory profile of some elected compounds in human whole blood (HWB) model

Compound	Dose (μmol/kg)	Δ Volume[a] (μL)	Inhibition (%)	ED_{50} (μmol/Kg)	HWB (PGHS-2) IC_{50} (μM)[c]
Vehicle	—	520.8 ± 17.8	—	—	—
(**1**) Celecoxib	100	364.1 ± 36.7	30.0*	87.7	2.9
(**3a**)	100	346.5 ± 51.1	33.4*	—	18.5
(**3c**)	100	260.7 ± 33.0	49.9*	11.5	—
(**3e**)	100	187.8 ± 23.7	63.9*	14.5	ns[b]
(**3i**)	100	373.9 ± 41.3	28.2*	—	—
(**3j**)	100	303.2 ± 52.7	41.7*	8.7	2.8
(**3l**)	100	431.3 ± 67.8	17.2 ns[b]	—	—
(**3m**)	100	424.0 ± 35.8	18.5 ns[b]	—	—
(**3n**)	100	511.3 ± 47.5	1.8 ns[b]	—	—

Compounds were administered orally; $N = 7–10$ animals.
[a] Results expressed in terms of mean ± SEM.
[b] Not statistically significant.
[c] Determined through the measurement of TXB_2 production derived from LPS-induced PGHS-2.
* $p < 0.05$ (ANOVA one way followed by Dunnet test).

2.3. Anti-hyperalgesic activity

The well-known involvement of peripheral p38 MAPK in hyperalgesic states induced by activation of vanniloid receptors led to the evaluation of the in vivo antinociceptive profile of 3-arylamine-imidazo[1,2-*a*]pyridine compounds in the capsaicin-induced thermal hyperalgesia model.[26] The title compounds (**3**), celecoxib (**1**) and p38 MAPK inhibitor SB203580 (**2**), used as reference compounds, were administered orally at the dose of 100 μmol/kg. The analysis of the obtained results disclosed in Figure 4 show that only compounds (**3j**) and (**3i**) have no effect on capsaicin-induced thermal hyperalgesia. All the other compounds tested are effective as anti-hyperalgesic agents.

Among the most active imidazo[1,2-*a*]pyridine derivatives, (**3a**), (**3l**) and (**3n**) presented bioprofile comparable to selective p38 MAPK inhibitor SB-203580 (**2**). The first is able to reverse completely the capsaicin-induced thermal hyperalgesia (Fig. 4A). The analgesic activity observed for derivative (**3a**) indicated the importance of the 2-pyridinil subunit attached to the heterocyclic central core, as the activity was significantly reduced when this group was replaced by the isosteric 4-pyridinyl or phenyl rings in compounds (**3e**) or (**3c**), respectively. Moreover, the comparison of the bioprofile of regioisomers (**3m**) and (**3l**) in the exploited hyperalgesy model led to the conclusion that the connection of 2-pyridinil group at the amine group instead of C-2 atom of the imidazo[1,2-*a*]pyridine scaffold is more favorable to the analgesic activity, once that compound (**3m**) is more active than compound (**3l**) (Fig. 4F vs Fig. 4G). This profile is probably resultant from the greater conformational flexibility of 2-pyridinil subunit of (**3l**) in comparison with (**3m**), where the nitrogen atom of this heterocyclic subunit forms an intramolecular hydrogen bond with the vicinal NH group, contributing to the conformational constraint of this derivative (Fig. 5).

The results obtained from this pharmacological assay indicate a possible action towards the p38 MAPK pathway, since inhibitors of the activity or the activation of the p38 MAPK enzyme can revert the capsaicin-induced thermal hyperalgesia.

Additionally, these results showed that the selective PGHS-2 inhibitor, celecoxib (**1**), does not have significant activity in this model, except for a low activity after 10 min from the beginning

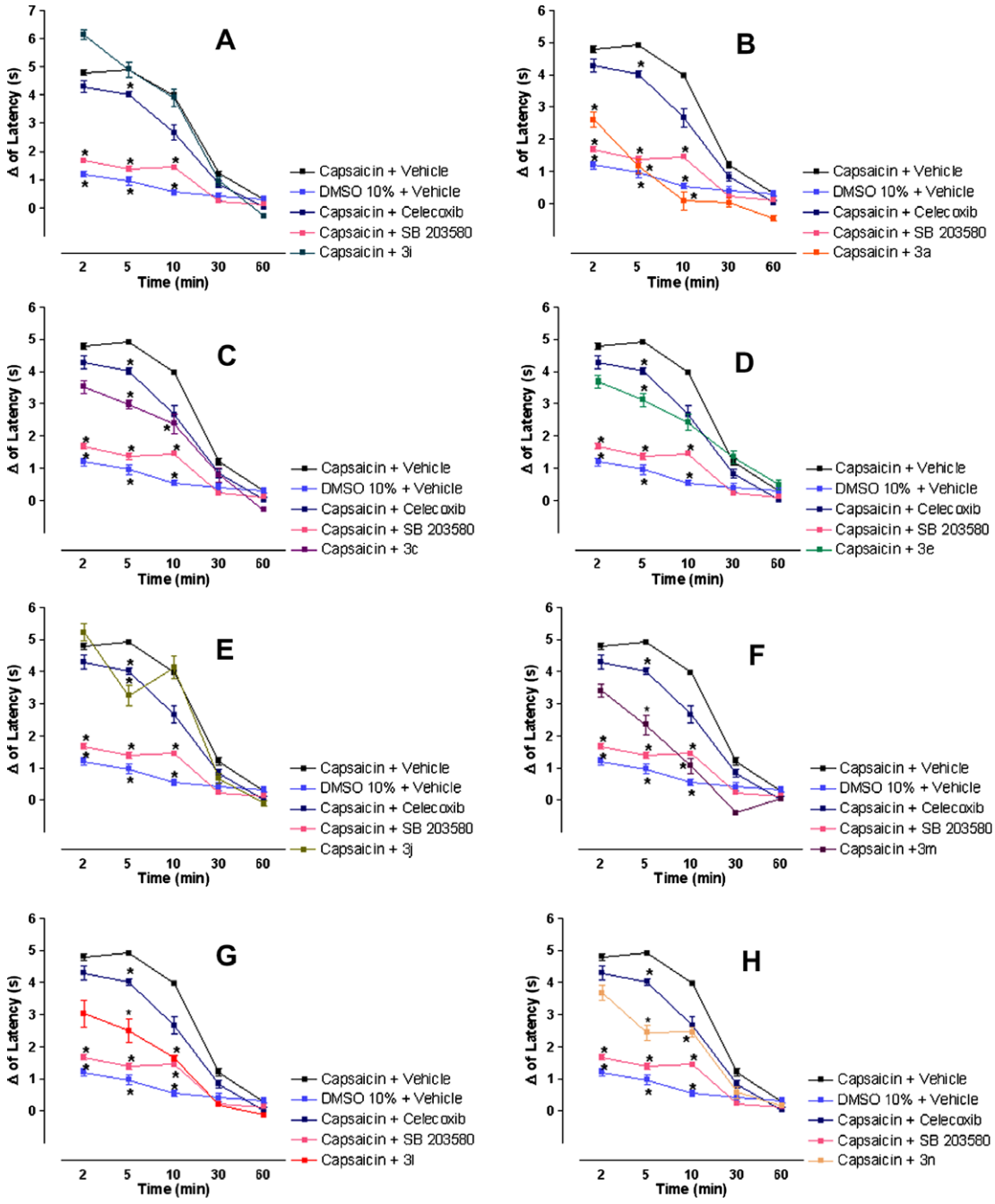

Figure 4. Time course effect of compounds (**3i**) (A), (**3a**) (B), (**3c**) (C), (**3e**) (D), (**3j**) (E), (**3m**) (F), (**3l**) (G), (**3n**) (H) in the capsaicin-induced thermal hyperalgesia. Compounds were administered orally. $N = 7–10$ animals. $^{*}p < 0.05$ (ANOVA one way followed by Dunnet test).

of the experiment, showing that the reduction of prostanoids biosynthesis deriving from the PGHS-2 inhibition does not lead to the total or partial reversal of capsaicin-induced thermal hyperalgesia. Thus, we can conclude that the activity shown in this assay for derivatives (**3a**), (**3c**), (**3e**), (**3m**), (**3l**) and (**3n**) should not be attributed to an eventual inhibition of PGHS-2.

2.4. Docking studies

The complex generated by docking studies of (**3j**) with PGHS-2 and superimposition with the structure of the selective inhibitor, SC-558 (**17**), co-crystallized with PGHS-2,[27] illustrated in Figure 6, shows that compound (**3j**) can bind in the active site of this enzyme in a similar fashion as the pyrazolic prototype (**17**). Comparison of the interactions performed by SC-558 in the crystal and the docked structure of (**3j**) with PGHS-2 (Fig. 6) shows that the methyl sulfonyl group of (**3j**) hydrogen bonds to the amino acid residue His90, similarly to the pharmacophoric sulfonamide group pertaining to SC-558. Moreover, the methoxyl group hydrogen bonds to both Tyr355 and Arg120, in the same region where the trifluoromethyl group of SC-558 binds, through hydrogen bonding with Arg120. Additionally, the imidazo[1,2-*a*]pyridine ring is not positioned in the same region as the central pyrazolic core of SC-558. Instead, it is close to the *p*-Br-phenyl ring of SC-558 (**17**), in the aromatic region of the active site lined by aromatic amino acid residues such as Phe381, Tyr385 and Trp387, among others. This result suggests extra interactions of (**3j**) in this hydrophobic pocket and indicates an inverted pharmaco-

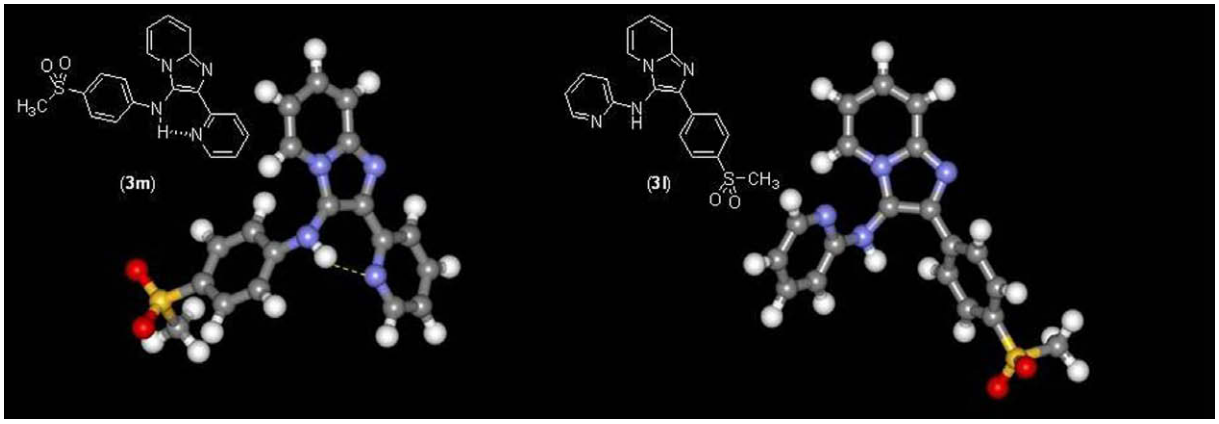

Figure 5. Minimum energy conformations obtained for compounds (**3m**) and (**3l**) by using the semi-empirical AM1 method.

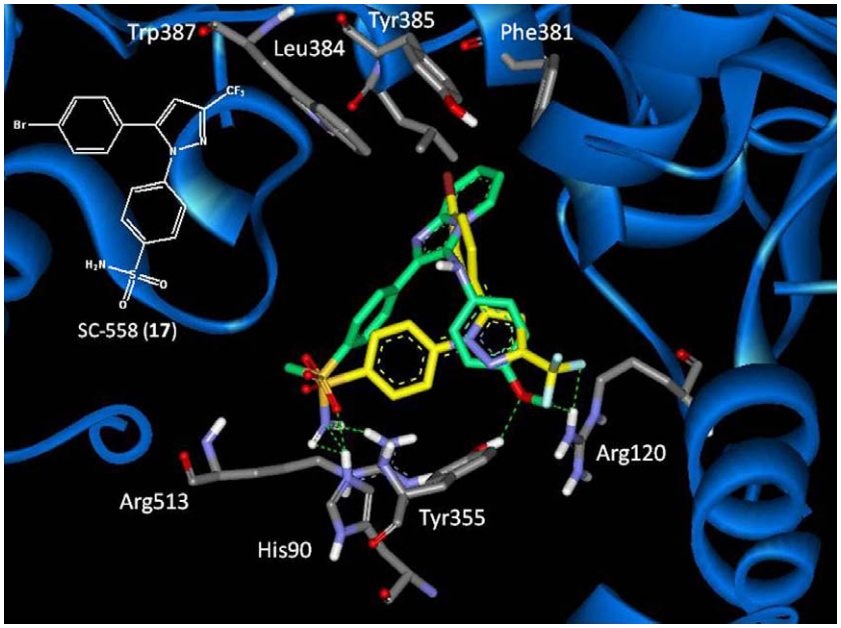

Figure 6. Representation of the top posing docked complex of (**3j**) (green carbon atoms) and the PGHS-2 inhibitor SC-558 (**17**) (yellow carbon atoms) in the active site of PGHS-2. Hydrogen bonds are shown as green dashed lines. Only polar hydrogens are shown for clarity.

phore compared to what has been described so far for PGHS-2 inhibitors. In short, the described interactions are typical of selective inhibitors of PGHS-2, confirming the molecular design of the reported class of analgesic and anti-inflammatory imidazo[1,2-*a*]pyridine derivatives (**3**).

3. Conclusions

The rational design of new imidazo[1,2-*a*]pyridine compounds based on the symbiotic approach, aiming at both p38-MAPK and PGHS-2 as therapeutic targets, was successful. Compound LASSBio-1135 (**3a**) was identified as a novel analgesic and anti-inflammatory orally-active prototype, acting through the inhibition of PGHS-2 and probably through the inhibition of the p38-MAPK pathway, proving to be a symbiotic drug candidate.

In addition, we observed that derivatives LASSBio-1140 (**3c**) and LASSBio-1141 (**3e**) were more active as antiedematogenic agents than celecoxib at the same molar dose and presented anti-hyperalgesic activity in the capsaicin-induced thermal hyperalgesia model. It is worth considering that the anti-inflammatory effect of LASSBio-1140 (**3c**) showed no relation to PGHS-2 inhibition, which opens a new possibility for further investigations of the pharmacological mechanism of action of these compounds.

Finally, it was also demonstrated that imidazo[1,2-*a*]pyridine derivative LASSBio-1145 (**3j**) is a novel PGHS-2 inhibitor, 10-fold more potent than celecoxib as an analgesic and an anti-inflammatory agent in the AcOH-induced abdominal constriction in mice (ED_{50} = 22.7 μmol/kg (8.9 mg/kg)) and carrageenan-induced rat paw edema (ED_{50} = 8.7 μmol/kg (3.4 mg/kg)) models. This result was corroborated by molecular docking studies with PGHS-2, which showed that this compound presents the pharmacophoric requisites for PGHS-2 inhibition.

4. Experimental

4.1. Chemistry

Reactions were routinely monitored by thin-layer chromatography (TLC) in silica gel (F245 Merck plates) and the products

visualized with iodine or ultraviolet lamp (254 and 365 nm). ^{1}H and ^{13}C nuclear magnetic resonance (NMR) spectra were determined in $CDCl_3$, DMSO-d_6 and trifluoroacetic acid-*d* (TFA) solutions using a Bruker AC-200 spectrometer. Peak positions are given in parts per million (δ) using tetramethylsilane as internal standard, and coupling constant values (*J*) are given in Hz. Infrared (IR) spectra were obtained using a Nicolet Magna IR 760 spectrometer. Samples were examined as potassium bromide (KBr) disks. Melting points were determined using a Quimis instrument and are uncorrected. Column chromatography purifications were performed using silica gel Merck 230–400 mesh. All described products showed ^{1}H and ^{13}C NMR spectra according to the assigned structures.

4.1.1. General procedure for preparation of *N*-arylformamides (8a–d)[17]

A round-bottomed flask fitted with a reflux condenser was fed with 49.5 mmol of the corresponding arylamines (**7a–d**) and 23.0 g (25 ml) of ethyl formate. The mixture was stirred and heated at reflux while 5.5 g (7.6 ml) of triethylamine was added, and afterward for another 24 h. After cooling at room temperature the reaction mixture was concentrated, followed by addition of water (50 ml). The obtained residue was submitted to extraction with dichloromethane (3× 40 ml). The organic layer was separated, dried over anhydrous sodium sulfate, filtered, and concentrated at reduced pressure to furnish the desired aromatic formamides (**8a–d**) as described next. All peaks in the 1H and 13C NMR spectra of these derivatives were doubled, due to restricted rotation about the amide bond as previously described by Krein and Lowary.[28]

4.1.1.1. 2-Pyridinylformamide (8a). Derivative (**8a**) was obtained in 35% yield, as a yellow solid, mp 34–36 °C. ^{1}H NMR (200 MHz, $CDCl_3$, δ): 10.31 (br s, 1H), 10.16 (br s, 1H), 9.31 (d, 1H, *J* = 8.1 Hz), 8.51 (s, 1H), 8.30–8.28 (m, 2H), 8.26 (d, 1H, *J* = 8.1 Hz), 7.80–7.60 (m, 2H), 7.06 (br s, 2H), 6.93 (d, 1H, *J* = 8.1 Hz); ^{13}C NMR (50 MHz, $CDCl_3$, δ): 163.2, 159.7, 151.1, 151.0, 148.5, 147.2, 139.1, 138.8, 120.2, 119.9, 115.3, 110.7. IR υ_{max} (KBr): 3197, 2852, 1691, 1595, 1433, 1303, 778, 517 cm^{-1}.

4.1.1.2. 4-(Methylthio)phenylformamide (8b). Derivative (**8b**) was obtained in 90% yield, as a white solid, mp 68–70 °C. ^{1}H NMR (200 MHz, $CDCl_3$, δ): 8.65 (s, 1H), 8.33 (s, 1H), 7.85 (s, 1H), 7.47 (d, 2H, *J* = 8.1 Hz), 7.23 (m, 4H), 7.03 (d, 2H, *J* = 8.1 Hz), 2.46 (s, 6H). ^{13}C NMR (50 MHz, $CDCl_3$, δ): 162.7, 159.1, 135.1, 134.3, 134.2, 134.2, 128.3, 127.7, 120.6, 119.5, 16.4; IR υ_{max} (KBr): 3310, 2916, 2866, 1715, 1683, 1527, 1308, 814, 516 cm^{-1}.

4.1.1.3. 4-(Methoxy)phenylformamide (8c). Derivative (**8c**) was obtained in 95% yield, as a white solid, mp 62–64 °C. ^{1}H NMR (200 MHz, $CDCl_3$, δ): 8.86 (br s, 1H), 8.50 (br s, 1H), 8.36 (br s, 1H), 8.25 (br s, 1H), 7.43 (d, 2H, *J* = 8.5 Hz), 7.02 (d, 2H, *J* = 8.5 Hz), 6.83 (m, 4H), 3.77 (s, 3H), 3.74 (s, 3H); ^{13}C NMR (50 MHz, $CDCl_3$, TMS) δ (ppm): 159.1, 157.2, 156.2, 129.8, 129.4, 121.5, 121.1, 114.5, 113.8, 55.1. IR υ_{max} (KBr): 3251, 3057, 2885, 1672, 1497, 1303, 1022, 833, 689, 517 cm^{-1}.

4.1.1.4. Phenylformamide (8d). Derivative (**8d**) was obtained in 80% yield, as a yellow solid, mp 34–36 °C. ^{1}H NMR (200 MHz, $CDCl_3$, δ): 9.13 (br s, 1H), 8.78 (br s, 1H), 8.38 (br s, 2H), 7.60–7.57 (m, 2H), 7.42–7.31 (m, 4H), 7.26–7.05 (m, 4H); ^{13}C NMR (50 MHz, $CDCl_3$, δ): 162.7, 159.3, 136.7, 136.5, 129.3, 128.7, 124.9, 124.4, 119.8; IR υ_{max} (KBr): 3264, 3057, 2874, 1695, 1597, 1442, 1311, 753, 541 cm^{-1}.

4.1.2. Alternative procedure for preparation of 2-pyridinylformamide (8a)[18]

Formic acid (0.8 ml, 22 mmol) and acetic anhydride (2.0 ml, 22 mmol) were mixed and stirred at 50–60 °C for 2 h. After cooling this mixture to room temperature, 2-aminopyridine (0.93 g, 10 mmol) was added in portions. Then, ethyl ether (30 ml) was added and the mixture was allowed to stir for another 48 h at room temperature. Then, the solvent was concentrated under reduced pressured, followed by the addition of 10% aq $NaHCO_3$ (30 ml) solution to the obtained residue and extraction with dichloromethane (3× 30 ml). The organic layer was separated, dried over anhydrous sodium sulfate, filtered, and concentrated at reduced pressure to furnish 2-pyridinylformamide (**8a**) (0.94 g) in 78% yield. The spectroscopic data of the samples of compound (**8a**) obtained from this methodology are in agreement with those previously described.

4.1.3. General procedure for preparation of arylisonitriles (6a–d)[16,17]

A round-bottomed flask equipped with a thermometer and a pressure-equalizing dropping funnel bearing a nitrogen inlet was charged with 40 mmol of the corresponding arylformamide derivative (**8a–d**), 13.8 ml of triethylamine and 40 ml of dichloromethane. After the resulting solution was stirred and cooled to −2° using an ice-salt bath, 3.7 ml of phosphorus oxychloride was added dropwise over 15–20 min, while the temperature was kept at 0°. The mixture became reddish brown as it was stirred and cooled at 0° for another hour. Then, ice–salt bath was removed and replaced by an ice–water bath. Stirring was continued while a 10% aq Na_2CO_3 solution (40 ml) was added dropwise at such a rate that the temperature of the mixture was maintained at 25–30 °C. The two-phase mixture was stirred for another 30 min, after which water was added until the volume of the aqueous layer was brought to 100 ml. The aqueous layer was separated and extracted with dichloromethane (3× 80 ml). The organic layers were combined, dried over anhydrous sodium sulfate and evaporated under reduced pressure to furnish the desired aromatic isonitriles (**6a–d**) as a crude oil, which were immediately used in the '3CC' step without further purification.

4.1.4. General procedure for preparation of 3-arylamino-imidazo[1,2-*a*]pyridines (3a–h) using classical '3CC' methodology[14]

Equimolar amounts of aromatic aldehyde, 2-aminopyridine and arylisonitrile (1 mmol) were dissolved in 3 ml of methanol, followed by addition of 2 mmol of glacial acetic acid. The resulting mixture was stirred at room temperature for 24 h then acidified with 1 N HCl until pH 1 and stirred for 30 min to destroy the residual isonitrile. After concentration of the reaction mixture under reduced pressure, 10% aq $NaHCO_3$ solution (15 ml) was added to the obtained residue, followed by extraction with ethyl acetate (3× 50 ml). The solvent was evaporated under reduced pressure. The organic layer was combined, dried over anhydrous sodium sulfate, filtered, and concentrated at reduced pressure to furnish the desired 3-arylamino-imidazo[1,2-*a*]pyridine derivatives (**3a–h**) as described next.

4.1.4.1. 2-Phenyl-*N*-(2-pyridinyl)imidazo[1,2-*a*]pyridin-3-amine (3a). Derivative (**3a**) was obtained in 40% yield, by condensation of 2-aminopyridine (**9**), phenylisonitrile (**6d**) and 2-pyridinylcarboxaldehyde (**10**), as a yellow solid, mp 235–237 °C. ^{1}H NMR (200 MHz, $CDCl_3$, δ): 8.55 (d, 1H, *J* = 4.4 Hz), 8.29 (s, 1H), 8.18 (d, 1H, *J* = 8.0 Hz), 7.75 (td, 1H, *J* = 7.8 and 1.6 Hz), 7.69–7.60 (m, 2H), 7.26–7.10 (m, 4H), 6.91 (t, 1H, *J* = 7.3 Hz), 6.75 (t, 1H, *J* = 7.3 Hz), 6.65 (d, 2H, *J* = 7.8 Hz); ^{13}C NMR (50 MHz, $CDCl_3$, δ): 154.3, 148.7,

143.4, 141.3, 136.5, 131.8, 129.3, 125.2, 123.9, 123.8, 121.4, 120.8, 120.7, 117.8, 116.6, 111.8; IR υ_{max} (KBr): 3207, 2951, 1601, 1560, 1387, 1237, 833, 750, 698 cm^{-1}.

4.1.4.2. 2-(4-(Methylthio)phenyl)-*N*-(2-pyridinyl)imidazo[1,2-*a*]pyridin-3-amine (3b). Derivative (**3b**) was obtained in 40% yield, by condensation of 2-aminopyridine (**9**), 4-(methylthio)phenylisonitrile (**6b**) and 2-pyridinylcarboxaldehyde (**10**), as a yellow solid, mp 154–156 °C. ^{1}H NMR (200 MHz, $CDCl_3$, δ): 8.53 (d, 1H, J = 4.8 Hz), 8.27 (s, 1H), 8.18 (d, 1H, J = 8 Hz), 7.73 (td, 1H, J = 7.8 and 1.7 Hz), 7.68–7.55 (m, 2H), 7.26–7.08 (m, 4H), 6.73 (t, 1H, J = 6.7 Hz), 6.59 (d, 2H, J = 8.6 Hz), 2.66 (s, 3H); ^{13}C NMR (50 MHz, $CDCl_3$, δ): 154.6, 149.0, 142.0, 136.9, 132.2, 130.1, 129.4, 125.3, 124.2, 124.0, 121.8, 121.0, 118.2, 117.6, 112.2, 18.0; IR υ_{max} (KBr): 3306, 3020, 1597, 1493, 1387, 1237, 750, 689 cm^{-1}.

4.1.4.3. *N*,2-Diphenyl-imidazo[1,2-*a*]pyridin-3-amine (3e). Derivative (**3e**) was obtained in 25% yield, by condensation of 2-aminopyridine (**9**), phenylisonitrile (**6d**) and benzaldehyde (**12**), as a white–green solid, mp 232–234 °C. ^{1}H NMR (200 MHz, DMSO-d_6, δ): 8.21 (s, 1H), 8.04 (d, 2H, J = 7.2 Hz), 7.92 (d, 1H, J = 6.7 Hz), 7.61 (d, 1H, J = 9.0 Hz), 7.41–7.26 (m, 4H), 7.12 (t, 2H, J = 7.6 Hz), 6.91 (t, 1H, J = 6.7 Hz), 6.71 (t, 1H, J = 7.2 Hz), 6.49 (d, 2H, J = 7.8 Hz); ^{13}C NMR (50 MHz, DMSO-d_6, δ): 145.1, 141.4, 137.0, 133.2, 129.1, 128.0, 127.1, 126.0, 124.8, 122.6, 118.5, 118.2, 116.6, 112.5, 111.9; IR υ_{max} (KBr): 3179, 2983, 2910, 1599, 1562, 1495,1387, 774, 751, 689 cm^{-1}.

4.1.4.4. 2-(4-(Methylthio)phenyl)-*N*-phenyl-imidazo[1,2-*a*]pyridin-3-amine (3f). Derivative (**3f**) was obtained in 50% yield, by condensation of 2-aminopyridine (**9**), phenylisonitrile (**6d**) and 4-(methylthio)benzaldehyde (**13**), as a white solid, mp 232–234 °C. ^{1}H NMR (200 MHz, TFA, δ): 8.91 (d, 1H, J = 6.2 Hz), 8.51–8.49 (m, 2H), 8.26 (d, 2H, J = 8 Hz), 7.99 (br s, 1H), 7.90–7.79 (m, 4H), 7.52–7.21 (m, 3H), 3.02 (s, 3H); ^{13}C NMR (50 MHz, TFA, δ): 145.6, 145.4, 140.0, 137.3, 132.4, 132.38, 129.6, 129.0, 127.6, 125.5, 123.5, 120.3, 119.8, 114.2, 108.0, 15.6; IR υ_{max} (KBr): 3156, 2983, 2910, 1597, 1487, 1387, 1354, 1254, 1097, 828, 751, 691, 508 cm^{-1}.

4.1.4.5. 2-(4-(Methylthio)phenyl)-*N*-(4-methoxyphenyl)-imidazo[1,2-*a*]pyridin-3-amine (3g). Derivative (**3g**) was obtained in 68% yield, by condensation of 2-aminopyridine (**9**), 4-methoxyphenylisonitrile (**6c**) and 4-(methylthio)benzaldehyde (**13**), as a white solid, mp 184–186 °C. ^{1}H NMR (200 MHz, DMSO-d_6, δ): 8.01 (d, 2H, J = 8.1 Hz), 7.92 (br s, 2H), 7.59 (d, 1H, J = 8.7 Hz), 7.27 (d, 3H, J = 7.8 Hz), 6.89 (t, 1H, J = 6.7 Hz), 6.75 (d, 2H, J = 8.7 Hz), 6.43 (d, 2H, J = 8.7 Hz), 3.62 (s, 3H), 2.46 (s, 3H). ^{13}C NMR (50 MHz, DMSO-d_6, δ): 152.1, 141.4, 138.9, 137.1, 136.7, 130.1, 126.6, 125.5, 124.7, 122.7, 119.2, 116.7, 114.8, 113.5, 111.8, 54.9, 14.3. IR υ_{max} (KBr): 3207, 2983, 1513, 1387, 1231, 1035, 828, 759, 508 cm^{-1}.

4.1.4.6. 2-(4-(Methylthio)phenyl)-*N*-(2-pyridinyl)-imidazo[1,2-*a*]pyridin-3-amine (3h). Derivative (**3h**) was obtained in 50% yield, by condensation of 2-aminopyridine (**9**), 2-pyridinylisonitrile (**6a**) and 4-(methylthio)benzaldehyde (**13**), as a light yellow solid, mp 233–235 °C. ^{1}H NMR (200 MHz, $CDCl_3$, δ): 8.88 (s, 1H), 7.99–7.94 (m, 3H), 7.87 (d, 1H, J = 6.8 Hz), 7.62–7.50 (m, 2H), 7.31–7.25 (m, 3H), 6.87 (t, 1H, J = 6.7 Hz), 6.71 (t, 1H, J = 6.2 Hz), 6.57 (d, 1H, J = 8.2 Hz), 2.46 (s, 3H); ^{13}C NMR (50 MHz, $CDCl_3$, δ): 156.8, 148.0, 141.6, 137.9, 137.2, 136.8, 130.3, 126.8, 125.5, 124.7, 123.1, 117.8, 116.7, 114.5, 111.8, 107.8, 14.5. IR υ_{max} (KBr): 3179, 2983, 2910, 1601, 1495, 1444, 1387, 1231, 1097, 828, 751, 698, 508 cm^{-1}.

4.1.4.7. Alternative two-step '3CC' procedure for preparation of 3-arylamino-imidazo[1,2-*a*]pyridine derivatives (3c) and (3d).[19] A solution of 2-aminopyridine (1 mmol) and 4-pyridinecarboxaldehyde (1 mmol) in toluene (15 ml) was heated at 50 °C for 30 min. Then, after addition of solid ammonium chloride (2 mmol) and the respective arylisonitrile derivative (1 mmol), the reaction mixture was refluxed for another 30 h. While still hot, the resulting dark brown solution was washed with warm water (50 ml), cooled down to room temperature and diluted with *n*-hexane (50 ml). The solvent was concentrated under reduced pressure and the desired product was obtained through acid–base extraction. The solid obtained was recrystalized from hexane–ethyl acetate (1:1) to furnish imidazo[1,2-*a*]pyridine derivatives as described next.

4.1.4.8. 2-(4-Pyridinyl)-*N*-phenyl-imidazo[1,2-*a*]pyridin-3-amine (3c). Derivative (**3c**) was obtained in 50% yield, by condensation of 2-aminopyridine (**9**), phenylisonitrile (**6d**) and 4-pyridinylcarboxaldehyde (**11**), as a brown solid, mp 208–210 °C. ^{1}H NMR (200 MHz, $CDCl_3$, δ): 8.49 (d, 2H, J = 5.4 Hz), 8.03 (d, 2H, J = 5.6 Hz), 7.94 (d, 1H, J = 6.8 Hz), 7.68 (d, 1H, J = 9.0 Hz), 7.38–7.27 (m, 3H), 7.23 (d, 1H, J = 9.0 Hz), 6.98–6.82 (m, 2H), 6.74–6.65 (m, 3H); ^{13}C NMR (50 MHz, $CDCl_3$, δ): 149.5, 144.0, 142.9, 141.1, 136.1, 129.9, 125.9, 121.0, 120.2, 120.2, 117.9, 113.4, 112.8; IR υ_{max} (KBr): 3246, 3029, 1601, 1493, 1391, 1240, 829, 801, 756 cm^{-1}.

4.1.4.9. 2-(4-Pyridinyl)-*N*-(4-(methylthio)phenyl)-imidazo[1,2-*a*]piridin-3-amine (3d). Derivative (**3d**) was obtained in 60% yield, by condensation of 2-aminopyridine (**9**), 4-(methylthio)phenylisonitrile (**6b**) and 4-pyridinylcarboxaldehyde (**11**), as a brown solid, mp 189–190 °C. ^{1}H NMR (200 MHz, DMSO-d_6, δ): 8.58 (d, 2H, J = 4.5 Hz), 8.42 (br s, 1H), 8.05–7.85 (m, 3H), 7.67 (d, 1H, J = 9.0 Hz), 7.36 (t, 1H, J = 7.8 Hz), 7.15 (d, 2H, J = 8 Hz), 6.96 (t, 1H, J = 6.5 Hz), 6.51 (d, 2H, J = 8.2 Hz), 2.35 (s, 3H); ^{13}C NMR (50 MHz, DMSO-d_6, δ): 149.4, 142.9, 141.6, 140.1, 134.1, 129.4, 125.6, 122.7, 120.4, 120.0, 117.0, 113.4, 112.3, 16.4; IR υ_{max} (KBr): 3207, 2951, 1632, 1601, 1513,1387, 1231, 828, 734, 689 cm^{-1}.

4.1.5. General procedure for preparation of arylsulfones (3i–n)[20]

A solution of 11.8 g of oxone® in 25 ml of water was added dropwise to a solution of 6.4 mmol of the corresponding arylsulfide derivative (**3b**), (**3d**) or (**3f–h**) in 25 ml of MeOH. The obtained mixture was stirred at room temperature for one hour when the TLC analysis indicated the end of the reaction, and then poured into an ice–water mixture. The resulting precipitate was filtered out, washed with water (15 ml) and air dried to furnish the desired arylsulfone derivatives (**3i–n**) as described next.

4.1.5.1. 2-(4-(Methylsulfonyl)phenyl)-*N*-phenyl-imidazo[1,2-*a*]-pyridin-3-amine (3i). Oxidation of arylsulfide derivative (**3f**) followed by purification on silica gel column using a mixture of hexane/AcOEt mixture as eluent furnished the compound (**3i**) in 60% yield, as white solid, mp >250 °C. ^{1}H NMR (200 MHz, DMSO-d_6, δ): 8.37 (s, 1H), 8.30 (d, 2H, J = 8.2 Hz), 7.99–7.93 (m, 3H), 7.66 (d, 1 H, J = 8.9 Hz), 7.35 (t, 1H, J = 8.2 Hz), 7.14 (t, 2H, J = 7.6 Hz), 6.95 (t, 1H, J = 6.6 Hz), 6.73 (t, 1H, J = 7.2 Hz), 6.51 (d, 2H, J = 7.8 Hz), 3.21 (s, 3H); ^{13}C NMR (50 MHz, DMSO-d_6, δ): 145.0, 142.0, 139.1, 138.5, 135.5, 129.5, 127.1, 126.7, 125.8, 123.2, 120.5, 118.8, 117.3, 112.9, 112.6, 43.4; IR υ_{max} (KBr): 3164, 3095, 2918, 2857, 1597, 1487, 1311, 1150, 958, 762, 541 cm^{-1}.

4.1.5.2. 2-(4-(Methylsulfonyl)phenyl)-*N*-(4-methoxyphenyl)-imidazo[1,2-*a*]pyridin-3-amine (3j). Oxidation of arylsulfide derivative (**3g**) followed by purification on silica gel column using a dichloromethane/MeOH mixture as eluent furnished the compound (**3j**) in 60% yield, as white–green solid, mp 180–182 °C. ^{1}H NMR (200 MHz, $CDCl_3$, δ): 8.36 (d, 2H, J = 8.4 Hz), 8.25 (s, 1H), 7.99 (d, 1H, J = 6.7 Hz), 7.80–7.55 (m, 4H), 7.13 (t, 1H, J = 6.7 Hz), 6.76 (d, 2H, J = 8.9 Hz), 6.60 (d, 2H, J = 8.9 Hz), 3.72 (s, 3H), 2.95 (s, 3H). ^{13}C NMR (50 MHz, $CDCl_3$, δ): 158.7, 150.0, 141.7, 137.5, 129.1, 129.5, 127.4, 125.5, 125.0, 122.6, 116.7, 115.9, 113.8, 112.1, 54.8, 44.9. IR υ_{max} (KBr): 3240, 2925, 2857, 1597, 1512, 1308, 1237, 1150, 958, 762, 541 cm^{-1}.

4.1.5.3. 2-(4-(Methylsulfonyl)phenyl)-*N*-(2-pyridinyl)-imidazo[1,2-*a*]pyridin-3-amine (3l). Oxidation of arylsulfide derivative (**3h**) followed by purification on silica gel column using a dichloromethane/MeOH mixture as eluent furnished the compound (**3l**) in 80% yield, as white solid, mp >250 °C. ^{1}H NMR (200 MHz, DMSO-d_6, δ): 9.04 (s, 1H), 8.26 (d, 2H, J = 8.5 Hz), 7.94 (d, 4H, J = 8.5 Hz), 7.67–7.54 (m, 2H), 7.34 (td, 1H, J = 0.8 and 6.7 Hz), 6.92 (t, 1H, J = 6.7 Hz), 6.67 (d, 1H, J = 8.3 Hz), 6.74 (m, 1H), 3.21 (s, 3H); ^{13}C NMR (50 MHz, DMSO-d_6, δ): 156.1, 147.6, 141.5, 138.6, 138.2, 137.6, 134.8, 126.7, 126.3, 125.1, 123.1, 119.3, 116.7, 114.4, 111.9, 107.7, 43.0; IR υ_{max} (KBr): 3142, 2920, 1700, 1601, 1476, 1310, 1147, 772, 536 cm^{-1}.

4.1.5.4. 2-(2-Pyridinyl)-*N*-(4-(methylsulfonyl)phenyl)-imidazo[1,2-*a*]pyridin-3-amine (3m). Oxidation of arylsulfide derivative (**3b**) followed by purification on silica gel column using a dichloromethane/MeOH mixture as eluent furnished the compound (**3m**) in 60% yield, as yellow solid, mp 227–230 °C. ^{1}H NMR (200 MHz, DMSO-d_6, δ): 9.0 (s, 1H), 8.52 (d, 1H, J = 3.9 Hz), 8.13 (d, 1H, J = 7.9 Hz), 7.93 (d, 1H, J = 6.8 Hz), 7.86 (td, 1H, J = 1.7 and 7.7 Hz), 7.70–7.54 (m, 3H), 7.36–7.24 (m, 1H), 6.97 (t, 1H, J = 6.7 Hz), 6.63 (d, 2H, J = 8.6 Hz), 3.06 (s, 3H); ^{13}C NMR (50 MHz, DMSO-d_6, δ): 151.3, 148.7, 147.6, 140.0, 135.0, 134.7, 127.8, 127.3, 123.9, 121.7, 120.7, 119.7, 118.2, 116.0, 111.5, 111.2, 42.5; IR υ_{max} (KBr): 3133, 2900, 2800, 1591, 1505, 1400, 1288, 1145, 772, 543, 530 cm^{-1}.

4.1.5.5. 2-(4-Pyridinyl)-*N*-(4-(methylsulfonyl)phenyl)-imidazo[1,2-*a*]pyridin-3-amine (3n). Oxidation of arylsulfide derivative (**3d**) followed by purification on silica gel column using a dichloromethane/MeOH mixture as eluent furnished the compound (**3n**) in 85% yield, as brown crystals, mp 194–196 °C. ^{1}H NMR (200 MHz, DMSO-d_6, δ): 9.12 (s, 1H), 8.59 (d, 2H, J = 6.4 Hz), 8.03 (d, 1H, J = 6.4 Hz), 7.93 (s, 2H), 7.70 (d, 3H, J = 7.9 Hz), 7.39 (t, 1H, J = 6.8 Hz), 6.99 (t, 1H, J = 6.2 Hz), 6.70 (d, 2H, J = 7.2 Hz), 3.09 (s, 3H); ^{13}C NMR (50 MHz, DMSO-d_6, δ): 146.9, 149.6, 142.3, 140.3, 134.8, 130.2, 129.2, 126.1, 123.2, 120.3, 119.2, 117.5, 113.1, 112.8, 44.0; IR υ_{max} (KBr): 3201, 3034, 2962, 2918, 1594, 1503, 1415, 1310, 1296, 1145, 958, 831, 750, 525 cm^{-1}.

4.2. Pharmacology

4.2.1. Acetic acid-induced abdominal constriction in mice[22]

The antinociceptive activity was determined in vivo using swiss mice (18–23 g) abdominal constriction test induced by acetic acid 0.6% (0.1 ml/10 g; ip). Test compounds (**3**) and celecoxib (**1**) were administered orally at a dose of 100 μmol/kg, as a suspension in 5% arabic gum in saline (vehicle). After 1 h, acetic acid was injected as previously described and 10 min after, the number of constrictions per animal was recorded for 20 min. The control animal received an equal volume of vehicle. Analgesic activity was expressed as percentage of inhibition of constrictions when compared with the vehicle control group. Results are expressed as the mean ± SEM of n animals per group.

4.2.2. Carragenaan-induced rat paw edema assay[23]

Fasted Wistar rats of both sexes (150–200 g) were used. The anti-inflammatory activity was determined in vivo using the carrageenan induced rat paw edema test (CIRPE). Test compounds (**3**) and celecoxib (**1**) were orally administered at a dose of 100 μmol/kg, as a suspension in 5% arabic gum in saline (vehicle). The control animals received an equal volume of vehicle. After 1 h, animals were then injected subplantarly with either 0.1 ml of 1% carrageenan solution in saline (0.1 mg/paw) into the right hind paws and sterile saline (NaCl 0.9%) into the left hind paws. Three hours after the subplantar injection, the paw volumes were measured using a glass plethysmometer coupled to a peristaltic pump. The edema was calculated as the volume difference between the carrageenan and saline-treated paw. Anti-inflammatory activity was expressed as percentage of inhibition of the edema when compared to the vehicle group control. Results are expressed as the mean ± SEM of n animals per group.

4.2.3. Capsaicin-induced hyperalgesia[26]

The anti-hyperalgesic activity was investigated using the capsaicin-induced thermal hyperalgesia test adapted from Mizushima et al.[26] Animals (fasted Wistar rats of both sexes (150–200 g)) were placed in a hot plate apparatus (Ugo Basile, Model-DS 37) at a temperature of 52 ± 0.1 °C to record the acclimatization and the basal latency of the withdrawal response. Then, test compounds (**3**), celecoxib (**1**) and SB203580 (**2**) were administered at a dose of 100 μmol/kg. After 1 h, 0.1 ml of 5% capsaicin solution in DMSO (5 μg/paw) was injected into animals' the right hind paws. The withdrawal latency of the right hind paw was determined at 2, 5, 10, 30 and 60 min post-challenge with a chronometer. The basal latencies were found to be 10–16 s. A cut-off time of 21 s was established to prevent any injury in the paw.

4.2.4. Determination of the inhibition of PGHS[25]

To evaluate the action of the compounds onto PGHS-1, fresh blood was collected into tubes containing no anticoagulant from normal volunteers who had not ingested any drugs within the previous two weeks. Blood aliquots were incubated with the compounds or vehicle (DMSO) at 37 °C for 1 h under constant agitation. At the end of incubation, the serum was obtained by centrifugation (6500 rpm for 10 min) and was tested for thromboxane B_2 production using an enzyme immunoassay kit (Amersham Biosciences) according to the manufacturer's instructions.

To evaluate the action of the compound onto PGHS-2, fresh blood was collected in heparinized tubes from normal volunteers as previously described. Aliquots of blood were incubated with the compounds or vehicle (DMSO) for 15 min at 37 °C under constant agitation. After that, the blood was incubated with 20 μL of lipopolysaccharide (LPS) solution at a final concentration of 10 μg/ml (SIGMA serotype 055:B5, diluted in phosphate buffer saline (PBS), pH 7.0) under constant agitation for 6 h at 37 °C in order to induce PGHS-2 expression. After incubation, the tubes were centrifuged at 6500 rpm for 10 min to obtain plasma that was frozen until the day of the assay. Plasma was tested for tromboxane B_2 production using an enzyme immunoassay kit (Amersham Biosciences) according to the manufacturer's instructions.

4.2.5. Docking studies

The molecular docking studies with PGHS-2 were performed using the flexible molecular docking software FlexE.[29]

4.2.6. Selection of protein crystal structures

Ligand-bound crystallographic structures of PGHS-2 are available in the Protein Data Bank.[30] In this study, crystal structures 1CX2, 4COX, 6COX were evaluated and selected for docking.[27]

4.2.7. Preparation of the ligands

The preparation of the ligands for FLExE was performed as for FLExX,[31] using Sybyl version 7.3.[32] First, the ligand coordinates were generated using the program Spartan Pro 1.0 for Windows (Wavefunction). Then, the correct atom types (including hybridization states) and correct bond types were defined and hydrogen atoms were added. Finally, systematic conformational analysis was performed with the semi empirical AM1 method[33] and the lowest-energy conformer was selected. In sybyl 7.3, Gasteiger-Hückel charges were assigned to the ligand database.[32]

4.2.8. Preparation of the ensemble protein structures

Proteins were prepared for the docking studies using the Biopolymer module of Sybyl 7.3. Amber7 FF99 charges were attributed to the protein atoms. Biopolymer protein analysis tool was used, in a stepwise process of analysis and correction of protein geometry parameters. Assignment of hydrogen positions has been made on the basis of default rules, available in Biopolymer. The side-chains of basic and acidic amino acid residues have been modeled in their ionized states and water molecules contained in the PDB file have been removed. Finally, the active site of the protein ensemble has been defined as the collection of residues within 10.0 Å of the bound inhibitor. All atoms located less than 10.0 Å from the ligand atoms were considered. Protein code number 1CX2 was used as a reference for the purpose of PGHS-2 docking with all compounds.

Acknowledgments

The authors acknowledge financial support and fellowships (to R.B.L., C.K.F.L., L.L.S., N.C.R., A.L.P.M., C.A.M.F., E.J.B.) from CAPES (BR), CNPq (BR), FAPERJ (BR), PRONEX (BR), and IM-INOFAR (BR, #420.015/05-1).

References and notes

1. Davies, S. P.; Reddy, H.; Caivano, M.; Cohen, P. *Biochem. J.* **2000**, *351*, 95.
2. Sherwood, E. R.; Toliver-Kinsky, T. *Best Pract. Res. Clin. Anaesthesiol.* **2004**, *18*, 385.
3. Melnikova, I. *Nat. Rev. Drug Discov.* **2005**, *4*, 453.
4. Mitchell, J. A.; Warner, T. D. *Nat. Rev. Drug Discov.* **2006**, *5*, 75.
5. Lee, J. C.; Laydon, J. T.; McDonnell, P. C.; Gallagher, T. F.; Kumar, S.; Green, D.; McNulty, D.; Blumenthal, M. J.; Heys, J. R.; Landvatter, S. W.; Strickler, J. E.; McLaughlin, M. M.; Siemens, I. R.; Fisher, S. M.; Livi, G. P.; White, J. R.; Adams, J. L.; Young, P. R. *Nature* **1994**, *372*, 739.
6. Badger, A. M.; Bradbeer, J. N.; Votta, B.; Lee, J. C.; Adams, J. L.; Griswold, D. E. *J. Pharmacol. Exp. Ther.* **1996**, *279*, 1453.
7. Lee, M. R.; Dominguez, C. *Curr. Med. Chem.* **2005**, *12*, 2979.
8. Morphy, R.; Kay, C.; Rankovic, Z. *Drug Discov. Today* **2004**, *9*, 641.
9. Fraga, C. A. M.; Barreiro, E. J. *Curr. Drug Ther.* **2008**, *2*, 13.
10. Duarte, C. D.; Barreiro, E. J.; Fraga, C. A. M. *Mini-Rev. Med. Chem.* **2007**, *7*, 1108.
11. Viegas-Junior, C.; Danuello, A.; Bolzani, V. D.; Barreir, E. J.; Fraga, C. A. M. *Curr. Med. Chem.* **2007**, *14*, 1829.
12. Colletti, S. L.; Frie, J. L.; Dixon, E. C.; Singh, S. B.; Choi, B. K.; Scapin, G.; Fitzgerald, C. E.; Kumar, S.; Nichols, E. A.; O'Keefe, S. J.; O'Neill, E. A.; Porter, G.; Samuel, K.; Schmatz, D. M.; Schwartz, C. D.; Shoop, W. L.; Thompson, C. M.; Thompson, J. E.; Wang, R. X.; Woods, A.; Zaller, D. M.; Doherty, J. B. *J. Med. Chem.* **2003**, *46*, 349.
13. Ribeiro, I. G.; da Silva, K. C. M.; Parrini, S. C.; de Miranda, A. L. P.; Fraga, C. A. M.; Barreiro, E. J. *Eur. J. Med. Chem.* **1998**, *33*, 225.
14. Groebke, K.; Weber, L.; Mehlin, F. *Synlett* **1998**, 661.
15. Passerini, M. *Gazz. Chim. Ital.* **1921**, *51*, 126.
16. Domling, A.; Ugi, I. *Angew. Chem., Int. Ed. Engl.* **2000**, *39*, 3169.
17. Hartman, G. D.; Weinstock, L. M. *Org. Synth.* **1988**, *50-9*, 620.
18. Guo, J. H.; Mayr, A. *Inorg. Chim. Acta* **1997**, *261*, 141.
19. Parchinsky, V. Z.; Shuvalova, O.; Ushakova, O.; Kravchenko, D. V.; Krasavin, M. *Tetrahedron Lett.* **2006**, *47*, 947.
20. Trost, B. M.; Curran, D. P. *Tetrahedron Lett.* **1981**, *22*, 1287.
21. Mandair, G. S.; Light, M.; Russell, A.; Hursthouse, M.; Bradley, M. *Tetrahedron Lett.* **2002**, *43*, 4267.
22. Collier, H. O. J.; Dinneen, L. C.; Johnson, C. A.; Schneide, C. *Br. J. Pharmacol.* **1968**, *32*, 295.
23. Ferreira, S. H. *Nat. New Biol.* **1972**, *240*, 200.
24. Lu, Z. H.; Xiong, X. Y.; Zhang, B. L.; Lin, G. C.; Shi, Y. X.; Liu, Z. G.; Meng, J. R.; Zhou, Y. M.; Mei, Q. B. *Acta Pharmacol. Sin.* **2005**, *26*, 1505.
25. Patrignani, P.; Panara, M. R.; Greco, A.; Fusco, O.; Natoli, C.; Iacobelli, S.; Cipollone, F.; Ganci, A.; Creminon, C.; Maclouf, J.; Patrono, C. *J. Pharmacol. Exp. Ther.* **1994**, *271*, 1705.
26. Mizushima, T.; Obata, K.; Yamanaka, H.; Dai, Y.; Fukuoka, T.; Tokunaga, A.; Mashimo, T.; Noguchi, K. *Pain* **2005**, *113*, 51.
27. Kurumbail, R. G.; Stevens, A. M.; Gierse, J. K.; McDonald, J. J.; Stegeman, R. A.; Pak, J. Y.; Gildehaus, D.; Miyashiro, J. M.; Penning, T. D.; Seibert, K.; Isakson, P. C.; Stallings, W. C. *Nature* **1996**, *384*, 644.
28. Krein, D. M.; Lowary, T. L. *J. Org. Chem.* **2002**, *67*, 4965.
29. Claussen, H.; Buning, C.; Rarey, M.; Lengauer, T. *J. Mol. Biol.* **2001**, *308*, 377.
30. Berman, H. M.; Westbrook, J.; Feng, Z.; Gilliland, G.; Bhat, T. N.; Weissig, H.; Shindyalov, I. N.; Bourne, P. E. *Nucleic Acids Res.* **2000**, *28*, 235.
31. Rarey, M.; Kramer, B.; Lengauer, T.; Klebe, G. *J. Mol. Biol.* **1996**, *261*, 470.
32. SYBYL 7.3 ed.; Tripos Inc.: 1699 South Hanley Rd, St. Louis, Missouri, 63144, USA.
33. Dewar, M. J. S.; Zoebisch, E. G.; Healy, E. F.; Stewart, J. J. P. *J. Am. Chem. Soc.* **1985**, *107*, 3902.